Piezoelectric Energy Harvesting: A Green and Clean Alternative for Sustained Power Production

Kimberly Ann Cook-Chennault, Nithya Thambi, Mary Anne Bitetto and E.B. Hameyie

Bulletin of Science Technology Society 2008; 28; 496
DOI: 10.1177/0270467608325374

Bulletin of Science, Technology & Society
Volume 28 Number 6
December 2008 496-509

10.1177/0270467608325374
http://bsts.sagepub.com
hosted at
http://online.sagepub.com

Piezoelectric Energy Harvesting

A Green and Clean Alternative for Sustained Power Production

Kimberly Ann Cook-Chennault
Rutgers University
Nithya Thambi
Mary Anne Bitetto
Rutgers University
E. B. Hameyie
Drexel University

Providing efficient and clean power is a challenge for devices that range from the micro to macro in scale. Although there has been significant progress in the development of micro-, meso-, and macro-scale power supplies and technologies, realization of many devices is limited by the inability of power supplies to scale with the diminishing sizes of CMOS-based technology. Here, the authors provide an overview of piezoelectric energy harvesting technology along with a discussion of proof of concept devices, relevant governing equations, and figures of merit. They present two case studies: (a) energy capture from the operation of a novel shear and elastic modulus indentation device subjected to applied voltage and (b) energy capture from vibrating commercial bimorph piezoelectric structures mounted on household appliances. Lastly, areas of development needed for realization of commercial energy harvesting devices are suggested.

Keywords: *piezoelectric; energy harvest; energy scavenge; power*

1. Introduction

Providing efficient and clean power is a challenge for devices that range from the micro to macro in scale. Although there has been significant progress in the development of micro-scale power supplies: combustors, solar cells, fuel cells, thermoelectric devices, and thin film and micro–batteries for portable micro electromechanical systems (MEMS), power management and consumption continue to be obstacles for the realization of many novel portable MEMS made up of complementary metal oxide systems (CMOS) because power consumption and the development of devices that power them do not adhere to Moore's Law. The *power challenge* is not limited to micro-scale devices where size and mass of conventional power supplies act as barriers to miniaturized portable electronics. Indeed, the U.S. industrial, transportation, and commercial sectors remain critical areas of investigation for power consumption of macro-scale devices due to the escalating cost of oil (the United States spent over $200 billion for oil imports in 2005; U.S. Department of Energy & U.S. Environmental Protection Agency, 2005) and effects of global warming and pollution (U.S. Department of Energy & U.S. Environmental Protection Agency, 2005). Despite notable efforts in the development and assessment of macro-scale sustainable energy technologies (e.g., solar cells, hydroelectric, wind, biofuels, and geothermal), approximately 86% of the energy consumed by the United States is derived from fossil fuel, and only 14% from renewables (U.S. Department of Energy & U.S. Environmental Protection Agency, 2005). And, the energy consumed by the United States continues to increase. The United States consumed 113.1 billion gallons of fuel in 2004, wherein 2,398 trillion (Energy Information Administration, 2002), 23,792 trillion (Energy Information Administration, 2006), and 9.86 quadrillion BTUs were consumed by the industrial, commercial, and residential sectors, respectively.

Here, we examine energy harvesting from external mechanical excitation, specifically piezoelectric energy-harvesting devices, which is becoming an area of increased interest. In Section 2, an overview of

piezoelectric energy-harvesting technology is presented along with a discussion of proof of concept devices, relevant governing equations, and figures of merit. In Section 3, opportunities for application of piezoelectric energy harvesting are described and two case studies are presented. The first case study focuses on capturing energy from the operation of a novel shear and elastic modulus indentation device subjected to applied voltage (Yegingil, Shih, & Shih, 2007). The second case study examines the amount of energy available from commercial bimorph piezoelectric structures when they are mounted (Yegingil et al., 2007) to household appliances. Section 4 provides an overview of areas that require advancement for the realization of commercial energy-harvesting devices. Section 5 follows with conclusions and future work.

2. Background

A plot of power density versus output voltage for common forms of regenerative power production is provided in Figure 1 (Beeby et al., 2007; Cook-Chennault, Thambi, & Sastry, 2008; Engel, Keawboonchuay, & Nunnally, 2000; Keawboonchuay & Engel, 2003, 2004; Miles, Hynes, & Forbes, 2005; Miles, Zoppi, & Forbes, 2007; Mitcheson et al., 2004; Mitcheson, Reilly, Toh, Wright, & Yeatman, 2007; O'Neill et al., 2003; Ramsay & Clark, 2001; Roundy, 2003; Roundy & Wright, 2004; Shearwood & Yates, 1997; Sodano, Inman, & Park, 2005a, 2005b; Sodano, Lloyd, & Inman, 2006; Umeda, Nakamura, & Ueha, 1996, 1997; White, Glynne-Jones, & Beeby, 2001; Xue, Uchida, Rand, & Forrest, 2004; see http://store.altenergystore.com/Solar-Panels/100-to-149-Watts-Solar-Panels/Mitsubishi-Electric-PV-MF110EC4-110W-Solar-Panel/p765/ and http://kensolar.com/tek9.asp?pg=products&specific=jnnscqr4&grp=). Piezoelectric devices possess power density values that are comparable to other regenerative energy technologies, such as lithium-ion batteries and electromagnetic power supplies, but possess less power density than advanced solar cells (high efficiency: ~25% at 100-1000 AM simulated solar intensity [mW/cm^2] subjected to optimal simulated sunlight). Thus, the purpose of this discussion is not to suggest that vibration-based energy scavenging is superior to other forms of regenerative energy systems but rather to elucidate the applications where this technology can be applied and suggest areas of needed improvement and investigation for enhancement of piezoelectric energy-harvesting devices.

Figure 1
This Plot of the Power Density Versus Voltage of Novel Regenerative Technologies Illustrates That, in Some Cases, Piezoelectric Energy Harvesting can Provide Power Density and Voltage Values That are Comparable to Lithium and Lithium-ion Secondary Battery Technologies

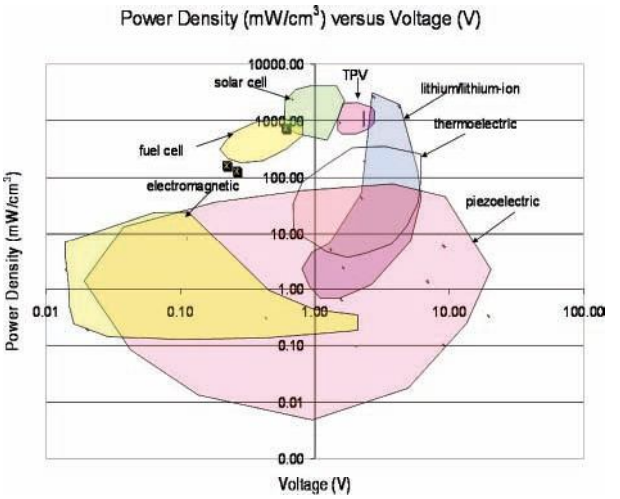

Piezoelectric materials produce an electrical potential when subjected to mechanical loads, and vice versa. Figures 2a through 2d (Cook-Chennault et al., 2008; Secretary, 1987; Yang, 2005) illustrate the direct piezoelectric process. In Figure 2a, an undisturbed molecular structure of the piezoelectric material is presented. In this figure, the positive and negative charges of each molecular gravity center cancel one another due to the molecular arrangement. Application of a force, F, to the molecular structure as depicted in Figure 2b causes the structure to deform, which thereby causes the positive and negative gravity centers to separate. Separation of the gravity centers within the molecular structure results in dipoles that polarize the material, as shown in Figure 2c. The polarized material consists of poles on the inside of the material that mutually cancel and positive and negative poles on the surface of the material (Secretary, 1987; Yang, 2005). The polarization effect is neutralized with the flow of free charge as shown in Figure 2d.

The linear constitutive equations that describe the mechanical and electrical behavior of piezoelectric materials are as follows (Secretary, 1987):

$$S_{ij} = s^{E}_{ijkl} T_{kl} + d_{kij} E_k \quad (1)$$

$$D_i = d_{ikl} T_{kl} + \varepsilon^{T}_{ik} E_k \quad (2)$$

Figure 2
(a) Undisturbed Molecular Structure, where Positive and Negative Charges Cancel, (b) Creation of Dipoles from Deformation of Molecular Structure Due to Applied Force, F, (c) Polarized Material, and (d) Neutralization of Polarization Effect from Flow of Electrons

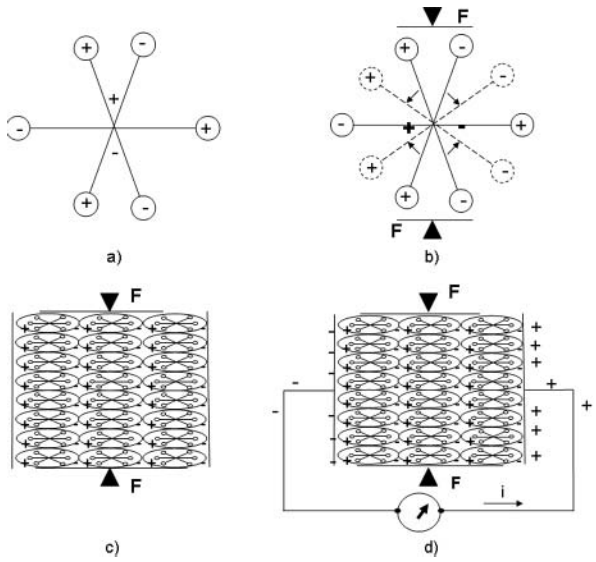

In Equations 1 and 2, subscripts i, j, k, and l take values of 1, 2, and 3. S and T are strain and stress tensors, respectively. T has SI units of N/m^2 and represents stresses that are induced by the mechanical and electrical effects. D and E are the electric displacement and electric field vectors, with SI units of C/m^2 and V/m, respectively. Also, s^E is the elastic compliance matrix evaluated at a constant electric field with SI units of m^2/N; d is a matrix of piezoelectric strain coefficients with SI units of m/V; and ε^T is a matrix of permittivity values that are evaluated at a constant stress with SI units of N/V^2. In Equations 1 and 2, d represents the charge created by a given force in the absence of an electric field (short circuit electrical condition) or the deflection caused by an applied voltage in the absence of an applied force (stress free mechanical condition) (Platt, Farritor, & Haider, 2005).

Thermal effects have also been included in the constitutive equations (Lee & Saravanos, 1998) for piezoelectric materials. These models are especially important for ferroelectric relaxor-type and composite materials because they behave nonlinearly with temperature and frequency. The thermo-piezoelectric constitutive equations at constant temperature and voltage that incorporate the coefficient of thermal expansion and pyroelectric effects are as follows:

$$S_{\varpi} = s_{\varpi\beta}^{E,T}(T)\sigma_{\beta} + d_{\varpi m}^{T}(T)E_m + \alpha_{\varpi}^{E,T}(T)\theta \tag{3}$$

$$D_m = d_{m\varpi}^{T}(T)\sigma_{\varpi} + \varepsilon_{mk}^{\sigma,T}(T)E_k + P_m^{\sigma,T}(T)\theta \tag{4}$$

where superscripts E, T, and α indicate constant voltage, temperature, and stress conditions, respectively, and ϖ and $\beta = 1, \ldots 6$, and k and $m = 1, 2$, and 3. The other values, P, s, S, T, d, E, α, θ, D, and ε represent the pyroelectric constant, elastic compliance tensor, strain, temperature, piezoelectric strain coefficient, electric field, coefficient of thermal expansion, temperature difference, electric displacement, and electric permittivity, respectively. Although a great deal of predictive models have been derived to evaluate the performance of piezoelectric materials, the majority of these have been for specific designs and have neglected temperature and nonlinear material responses.

Piezoelectric materials are typically described in terms of coupling coefficient, voltage coefficient, mechanical quality factor, energy, and efficiency. The coupling coefficient, k, is obtained from the expression

$$k^2 = \frac{d^2}{s\varepsilon} = \frac{d^2 Y}{\varepsilon}. \tag{5}$$

In Equation 5, Y is the Young's modulus. The effective electromechanical coupling factor, k_{eff} (H. W. Kim et al., 2004), for a composite piezoelectric material is obtained from the following expression:

$$k_{eff} = \sqrt{1 - \left(\frac{F_r}{F_\alpha}\right)^2}, \tag{6}$$

where F_r is the resonance frequency (Hz) and F_a is the antiresonance frequency (Hz) of a piezoelectric cantilever beam. The voltage coefficient, g (V-m/N) (H. W. Kim et al., 2004; Secretary, 1987), is expressed as

$$g = \frac{d}{\varepsilon^T}. \tag{7}$$

The mechanical quality factor, Q_M (Secretary, 1987), is defined as

$$Q_M = 2\pi \frac{\text{energy stored per cycle}}{\text{energy dissipated per cycle}}. \tag{8}$$

The amount of energy, E_C, stored in a piezoelectric element is

$$E_C = \frac{1}{2} CV^2, \tag{9}$$

where C is the capacitance of the piezoelectric source and V is the voltage produced (Shenck & Paradiso, 2001).

The efficiency of piezoelectric devices can be computed from two expressions (Cho, Anderson, Richards, Bahr, & Richards, 2005a, 2005b; Richards, Anderson, Bahr, & Richards, 2004). In Equation 10, the ability of the piezoelectric material to convert mechanical energy to electrical energy is expressed as a function of the coupling coefficient and mechanical quality factor. This expression (Richards et al., 2004) illustrates the influence of k and Q_m on the efficiency. Specifically, increasing k and Q_m results in an increase in device efficiency. Therefore, this form of efficiency is used in making material selection. This expression is also significant because it illustrates that reduction of the structural stiffness can lead to the largest gain in efficiency.

$$\eta = \frac{\frac{1}{2}\left(\frac{k^2}{1-k^2}\right)}{\frac{1}{Q_M} + \frac{1}{2}\left(\frac{k^2}{1-k^2}\right)}. \tag{10}$$

The other (Sodano et al., 2005a) expression for efficiency is based on a piezoelectric cantilever beam subjected to a vibration load,

$$\eta = \frac{P_{out}}{P_{in}} \times 100\% = \frac{1}{M}\sum_{n=2}^{M} \frac{(V_n + V_{n-1})^2/R}{[(F_n + F_{n-1}) \cdot (\delta_n - \delta_{n-1})]/(t_{n-t_{n-1}})} \times 100\%. \tag{11}$$

In Equation 11, V is the voltage drop across the load resistance, R, F is the force applied to the base of the cantilever beam, δ is the displacement of the beam, t is the time increment between captured data points, n is the data point index, and M is the total number of data points measured.

The piezoelectric effect is expressed in single crystals, ceramics, polymers, composites, thin films, and relaxor-type ferroelectric materials, but the majority of the energy-harvesting devices fabricated in past work have been made up of polymers (PVDF) and ceramics (lead zirconate-lead titanate, PZT). The most common types of mechanical loading investigated for piezoelectric energy-harvesting devices are 33 and 31 loading, which are depicted in Figures 3a and 3b (Roundy, Wright, & Rabaey, 2003), where x, y, and z axes are labeled 1, 2, and 3, respectively. In the 33 loading mode, the voltage and stress act in the same direction, and in the 31 mode, the voltage acts in the 3 direction, while the mechanical stress acts in the 1 direction. For devices with a rectangular cross-section, the poling direction is denoted as the 3 direction, and 33 loading refers to the collection of charge on the electrode surface perpendicular to the polarization direction when tensile or compressive mechanical forces are applied along the polarization axis. When a material experiences 31 loading, the charge is collected on the electrode surface perpendicular to the polarization direction, for example, when the force is applied perpendicular to the axis of polarization.

Figure 3
(a) 33 Loading Depicted, Wherein The Voltage and Stress Act in The Same Direction; (b) 31 Loading Depicted, Wherein the Loading and Stress Act in Opposing Directions

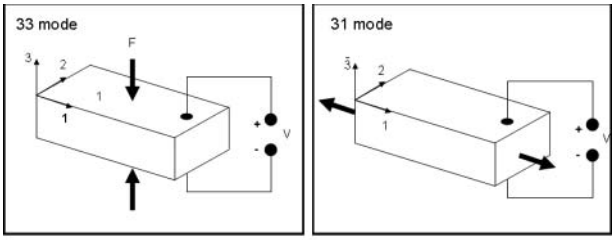

(a) (b)

Table 1 (Cook-Chennault et al., 2008; Engel et al., 2000; Jeon, Sood, Jeong, & Kim, 2005; H. W. Kim et al., 2004; Platt, Farritor, Garvin, & Haider, 2005; Priya, Chen, Fye, & Zahnd, 2005; Ramsay & Clark, 2001; Ren, Liu, Geng, Hofmann, & Zhang, 2006; Schmidt, 1992; Shenck & Paradiso, 2001; Whalen, Thompson, Bahr, Richards, & Richards, 2003; White et al., 2001) provides a detailed list of novel piezoelectric devices, along with their application, power, voltage, and current data. From Table 1, it can be seen that proof of concept devices developed in previous work have ranged in scale from micro to macro, with output power values that range from 1 μW to 29 kW. The majority of the prototype energy-harvesting devices have been for macro-scale applications, for example, windmills, wave energy, shoe inserts, and biomedical implants.

Three types of windmill designs have been constructed (Myers, Vickers, Kim, & Priya, 2007; Priya et al., 2005; Schmidt, 1992). One design consisted of PVF_2 bimorphs that were subjected to 33 compressive

Table 1
Novel Piezoelectric Devices and the Application, Size, Energy/Power Density, Voltage, and Applied Loading Conditions

Material	Application	Dimensions	Power	Energy / Power Density	Voltage	Load
PZT composite – d33 compressive loading of 39 Mpa	composite	-	-	12 mW/cm^3	-	-
PVF_2, d33 compressive load	wind mill rotor design	500 μm x 90 mm x 70 mm	2.4 μW	0.76 μW/cm^3	1 V	400 kΩ
PVDF bimorph, d31 mode	shoe insert	-	1.3 mW	-	18 V	250 kΩ
PZT dimorph, d31 mode	shoe insert	-	8.4 mW	-	64.8 V	500 kΩ
PVDF bimorph windmill, 12 cantilever bimorphs d31 loading	windmill	each bimorph: 60 x 20 x 0.5 mm^3	10.2 mW	1.42 mW/cm^3	6.8 V	4.6 kΩ
PZT-5A membrane, d31 loading from blood pressure	biomedical	surface area = 1cm^2 thickness = 9 μm	2.3 μW	2.6 mW/cm^3	-	-
PZT rectangular structure, knee implant, d33 compressive loading	knee implant	1.0 x 1.0 x 1.8 cm^3	4.8 mW	0.89 mW/cm^3	-	-
Unimorph membrane transducer subjected to shaker vibration	Low power sensors	Total radius = 20.5 mm, PZT radius = 12.5 mm, PZT thickness = 230 μm, bras thickness = 400μm	1.7mW	0.106mW/cm^3	9 V	47k Ω
PZT thin film d33 mode cantilever generator	MEMS	170 μm x 260 μm	1 μW	0.74 mWh/cm^2	2.2 V	5.2 MΩ
PZT thick film operating at 80 Hz	MEMS	20 μm thick layers	2 μW	-	0.816 V	333 kΩ
PZT with 1.5 MPa lateral stress operating at 15 Hz	Autonomous wireless transmitter	Volume =0.2 cm^3	1.2 mW	6 mW/cm^3	9 V	-
PZT stacked generator – 164 layers at 1 Hz subjected to 250 N	Power from activated muscle	5 mm x 5 mm x 8 cm	690 μW	345 μW/cm^3	19.3 V	540 kΩ
PZT thin film membrane generator coupled with heat engine	hybrid	surface area = 3mm^2 thickness = 3.4 μm	56 μW	5.5 W/cm^2	-	-
PZT cymbal device, d33 loading	cymbal	diameter = 29 mm thickness = 1 mm	29 mW	43.9 mW/cm^3	-	-
PZT projectile generator, d33 compressive loading	pulse generator	diameter = 1.27 cm thickness = 0.13 cm	25 kW	151.4 kW/cm^3	500 V	10 Ω
PMN-PT composite – d33 compressive loading of 40.4 MPa	composite	-	-	22.1 mW/cm^3	-	-
PZT, steel and brass drum actuator subjected to cyclic stress of 0.7 N at 590 Hz	-	Volume = 0.51 cm^3	11 mW	21.57 mW/cm^3	14.07	18 kΩ
Nanowire arrays of piezoelectric and semiconductive ZnO	Biosensors and self-powered electronics	300 nm diameter wire Array dimensions: 6.5 μm x 3.2 μm	~10-20 pW per wire	0.1-0.2 mW/cm^2	20 mV	

loading from rotation and mechanical oscillation from the wind. From this study, it was concluded that for compressive, 33-mode loading, higher oscillating frequencies were necessary and that this could be achieved by scaling down the oscillator size and increasing the number of oscillating devices. Another piezoelectric windmill design was made up of 12 PVDF piezoelectric bimorphs positioned along the circumference of the mill with cantilever supports. In this design, a traditional windmill was coupled with a piezoelectric device, wherein wind flow induced a camshaft gear mechanism to oscillate, thereby causing the bimorphs to deflect, resulting in electrical power. The third windmill design was created for

small-scale applications. This structure was made primarily of plastic and included 18 bimorphs. This windmill generated 5 mW of continuous power when subjected to an average wind speed of 10 miles per hour.

Several researchers have investigated energy generation from piezoelectric shoe inserts. One design was made up of two shoe inserts (Shenck & Paradiso, 2001) subjected to 31-mode loading, wherein one insert was a flexible PVDF bimorph placed under the shoe insole and the other was a dimorph structure consisting of a curved semiflexible PZT material laminated onto prestressed metal strips that was subjected to heel pressure. The workers concluded from this study that since the low-frequency piezoelectric sources were capacitive, they produced high-voltage, low-energy, and low-current pulses (10-7 A), which were an efficient means of conversion of mechanical to electrical energy, as long as adequate power conditioning was provided. The second shoe insert design (Mateu & Moll, 2005) was also made of a PVDF bimorph subjected to 31-mode loading conditions. These workers concluded that piezoelectric rectangular beams subjected to 31-mode loading conditions required high length-to-height ratios in order to produce maximum charge density. A third shoe insert design (Yoon, Washington, & Danak, 2005) was made up of a two-layer curved unimorph shoe insert and was modeled using shallow thin shell theory and linear piezoelectric constitutive equations. The model was used to identify the influence of thickness, length, width, and center height on maximum charge density. These workers found that the dimensions of the unimorph influenced its overall power production. Specifically, they found that increasing the width of the unimorph resulted in higher charge generation than increasing the length. They also concluded that increasing the center height and thickness of the substrate (limited by available input force) also enhanced the charge generation of the generator.

Several groups have investigated piezoelectric energy harvesting from implantable devices. In one study (Ramsay & Clark, 2001), PZT-5A, PZT-5H, and PVDF membranes were used to produce power from fluctuating blood pressure. Although the devices did produce power, the amount of power produced was insufficient for the proposed application. The workers concluded that further development of materials, signal processing, and device design were required for the realization of devices for adequate power production. A 33-mode PZT generator prototype for powering an orthopedic knee implant (Platt, Farritor, Garvin, et al., 2005; Platt, Farritor, & Haider, 2005) was evaluated for power production. Although the actual device was not implanted, it was subjected to lifetime studies. The results indicated a linear decrease in power per decade of operational time. A comparison of stacked versus monolithic elements of PZT was also investigated in this study, and it was concluded that elements with the same geometry produced the same output power, with matching loads. However, the stacked elements required lower matching electrical load requirements, resulting in lower output voltages, which were more manageable for real-world applications.

Devices, called Eels, have been fabricated to harvest energy from water movement (Allen & Smits, 2001; Taylor, Burns, Kammann, Powers, & Welsh, 2001). These devices were made up of PVDF beams that were placed in the wake of a bluff body in oceans and rivers. Preliminary studies indicate that larger scaled devices would produce power in the milliwatt and watt power ranges. Despite the vast number of prototype devices for energy harvesting, there are many other opportunities for commercial implementation of piezoelectric energy-harvesting devices. Therefore, we have dedicated Section 3 to a discussion of other opportunities for energy harvesting via piezoelectric energy-harvesting devices.

3. Opportunities for Energy Harvesting Using Piezoelectric Materials

Piezoelectric power generation can be divided into two categories: (a) self-energizing devices, for example, devices that are self-powered solely from static or dynamic movement of the piezoelectric device while acting as a sensor or actuator, and (b) energy-harvesting devices that are attached to existing structures that vibrate during operation of the structure. Both types of devices capture otherwise wasted mechanical loading and convert it to electrical power. Self-energizing piezoelectric devices are well suited for low power wireless and MEMS applications (Ramsay & Clark, 2001) due to their low power and current density requirements, while macro-scale devices and structures that routinely experience static and dynamic mechanical loading can potentially offer larger deflections and surface areas for arrays of devices. The opportunities for implementation of these devices commercially include, but are not limited to, the following:

1. self-energizing devices for health monitoring of bridges and structures
2. energy harvesting from static mechanical loading in cell phones, key pads, and touch screens
3. energy harvesting from transportation systems and household appliances
4. self-energizing and energy-harvesting biomedical implants, sensors, and medical diagnostic devices

Of these applications, we have chosen to briefly examine the application of these devices to bridges and automobiles and present two case studies on a biomedical device and three household appliances. Bridges experience two types of vibrations: free and forced vibrations. Free vibrations are due to internal movement of the structural members, while forced vibrations are induced by external forces such as traffic or wind. A forced vibration can be either lateral or torsional. Structural applications offer both self-energizing and energy scavenging opportunities. First, sensors used to monitor civil engineering structures can be designed to be self-energizing devices, and other devices may be attached to engineering structures for energy scavenging from free and forced vibrations that can ultimately contribute to grid power. Typically, vibrations are experienced in the deck of the bridge, and failure occurs when the external vibrations are at a frequency equal to the resonant frequency of the structure. Amplitudes and frequencies of vibrations depend on the bridge design and loading conditions during operation. In order to prevent bridge failures such as the Tacoma Bridge failure, routine structural health monitoring of bridges is performed, wherein vibration is recorded and fatigue analyses performed. The most prevalent methods of health monitoring of bridges include subjective incremental visual assessments or localized testing methods that utilize eddy current, ultrasound, acoustic bases sensing, and strain and corrosion monitoring. The majority of these techniques require sensors to measure parameters such as moisture content, rate of loading, loading time, stress/strain amplitude, deflection/displacement, acceleration/vibration, chemical composition, and temperature. We believe that the power generated from techniques such as electromechanical impedance (EMI) transducers (which include piezoelectric ceramic patches as impedance transducers mounted on bridge structures) can be stored in secondary batteries or supplied (with appropriate signal processing) to the grid.

Both static and dynamic mechanical loading are also encountered in the operation of automobiles. Examples of static loading include 33 loading from pressing key pads and user screen interfaces, acoustic vibrations from stereo and speaker cell phones, and vibration during driving and operation of the engine. Small-scale studies by auto manufacturers indicate that the highest vibrations, also referred to as highest noise regions, occur at the metal door panels, the car deck, and metal panels close to the speakers (C.-W. Kim, Jung, & Choi, 2008). Harmonic vibrations are the primary reason for fatigue in the car and an area of experimental modal analysis, but work to implement devices to harvest this energy has not, to our knowledge, been demonstrated.

Figure 4
Schematic Depicting the Piezoelectric Device Modeled. In Operation, Voltage is Applied to the top Layer of the Structure, while the Induced Voltage is Measured from the Bottom of the Device

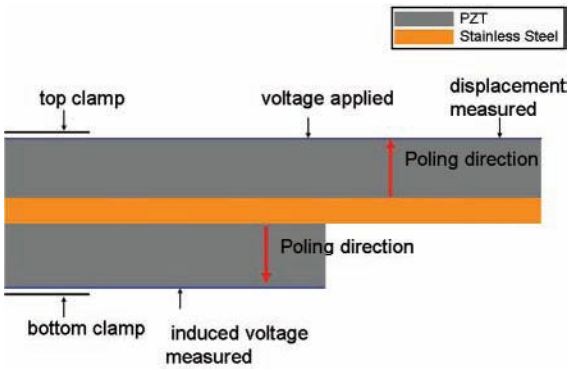

Table 2
Electrical and Mechanical Boundary Conditions for Three-Tiered Piezoelectric Device

Layer	Length (mm)	Width (mm)	Height (mm)
Top	31.3	9.6	0.127
Middle	31.3	9.6	0.05
Bottom	18.5	9.6	0.127
Boundary Condition	Value	Location	
Displacement	Fixed		
Electrical Charge	Ground		
Electrical Charge	Zero Charge/Symmetry		
Applied Voltage (V)	1 – 17 Volts		

Table 3
Material Properties Used for the PZT in the COMSOL Model

Elasticity Matrix (Pa)					
1.44e11	9.57e10	1.01e11	0	0	0
	1.44e11	1.01e11	0	0	0
		1.35e11	0	0	0
			2.30e10	0	0
				2.30e10	0
					2.39e10
Coupling Matrix (C/m^2)					
0	0	0	0	17.03	0
0	0	0	17.03	0	0
-10.86	-10.86	23.24	0	0	0
Compliance Matrix (1/Pa)					
16.5e-12	-4.78e-12	-8.45e-12	0	0	0
	16.5e-12	-8.45e-12	0	0	0
		20.7e-12	0	0	0
			43.5e-12	0	0
				43.5e-12	0
					42.6e-12
Coupling Matrix, Strain-charge form (C/N)					
0	0	0	0	741e-12	0
0	0	0	741e-12	0	0
-274e-12	-274e-12	593e-12	0	0	0
Relative Permittivity, stress-charge form					
1704.40		0		0	
		1704.40		0	
				902	
Relative Permittivity, strain-charge form					
3130		0		0	
		3130		0	
				3400	

Figure 5
Plot of Induced Voltage and Displacement Versus Applied Voltage. These Results Indicate That the Power Induced During the Operation of the Device can be Captured and Re-applied to the System

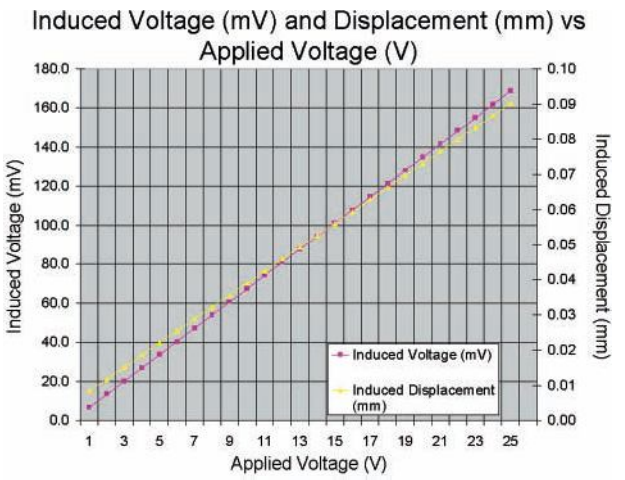

3.1 Case Studies

3.1.1 In vivo indentation shear and elastic modulus measurement device. Here, we provide a case study on a biomedical tissue indentation shear and elastic modulus measurement device developed by Yegingil et al. (2007). The device consists of two piezoelectric sheets that sandwich a stainless steel sheet, wherein a tip for in vivo applications is provided at the right end of the cantilever structure. We have simplified the device by removing the tip as shown in Figure 4. The top and bottom layers of the device are made of PZT-5H, while the middle layer is stainless steel. The boundary conditions for the models are provided in Table 2. The material properties used for PZT-5H are detailed in Table 3. All three layers are clamped at the left end, so that the device is mounted in a cantilever fashion. The top layer is the driving electrode. The second layer, which is composed of stainless steel, provides structural support and is used to perform the compression and shear tests on human tissue. The third layer is the sensing electrode. In operation mode, a driving voltage is applied to the top layer, while the induced voltage and output displacement of the tip are recorded to determine the elastic modulus of human tissue.

Using the COMSOL Multiphysics finite element MEMS modeling tool, we have created a 2D simplified model of the Yegingil et al. (2007) device. In this model, we have applied a voltage to the driving electrode and recorded the voltage induced in the sensing electrode, along with the maximum displacement of the top driving electrode. The dimensions and boundary conditions for the model are given in Table 2. A plot of applied voltage versus the induced voltage and displacement is provided in Figure 5. In this plot, the applied voltages range from 1 to 25 volts and the induced voltage and displacement range from ~7 to 170 mV and ~3 to 85 microns, respectively. The results demonstrate that the energy captured from the device during in vivo operation can be used to provide power to the device with the use of adequate signal processing.

3.1.2 Household appliances: Washer, dryer, and microwave. The second case study focuses on incorporation of energy-harvesting devices with common

Table 4
Energy Consumption, Hours of Operation per month, acceleration, and frequency for clothes dryer, washing machine, and Microwave oven

Appliance	Energy Consumption (kWh/month)	Operation (Hours/ Month)	Acceleration (m/s^2)	Frequency (Hz)
Clothes Dryer	74	25.8	3.5	121
Washing Machine	72 (hot and cold washes)	34.4	0.5	109
Microwave Oven	10	6.45	2.25	121

Table 5
Dimensions and Electromechanical Properties of Devices Studied

Piezoelectric Device		
	APC International, 40-1010	MIDE, qp20w
Dimensions: length, width, thickness (mm)	60 X 20 X 0.60	50.8 X 38.1 X 0.76 (actuator dimensions: 46 X 34.8 X 0.25)
Capacitance (μF)	0.17	0.20
Blocking force (N)	> 0.25	not given
Resonant frequency (Hz)	65	not given

Figure 6
Picture of the Shaker Assembly Setup, Wherein Actuators are Subjected to Loading Experienced by Household Appliances, and the Output Voltage Induced from the Dynamic Loading is Recorded as a Function of Time

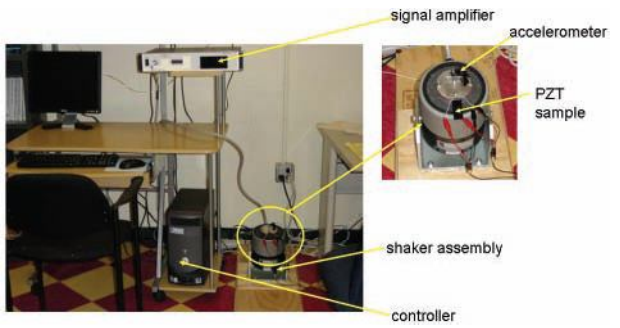

household appliances. A number of household devices experience both dynamic vibration and static loading via the pressing of key pads and force from operation. In our case study, we examine three household devices: a washing machine, clothes dryer, and microwave. Approximate values for hours of operation per month (APS, 2008), along with acceleration and frequency of these devices (Roundy, 2005), are provided in Table 4. We subjected a PZT stripe bimorph actuator (catalog number 10-1010), from APC International, and a PZT quickpack from MIDE (catalog number qp20w) to acceleration and frequency boundary conditions experienced by the household appliances described in Table 4.

Descriptions of the piezoelectric devices are provided in Table 5, and a schematic of the test setup is depicted in Figure 6. In Figure 6, a shaker assembly, signal amplifier, and control system are depicted. The piezoelectric device is clamped and mounted onto the shaker assembly and subjected to frequency and g-loads typically experienced by microwaves and clothes washers and dryers (provided in Table 4). The output voltages from both actuators were recorded as a function of time and are shown in Figures 7a and 7b.

The voltage obtained from the piezoelectric devices was used to calculate power provided from each device,

$$P_S = 2vi. \tag{12}$$

In Equation 12, v is the absolute value of the maximum voltage value obtained from sinusoidal vibration loading of the piezoelectric device, and i is the current in amps. Since the piezoelectric strips are bimorphs, the product of the voltage and current from the actuator is multiplied by a factor of 2 in Equation 12. The current for the actuator is computed from

$$i = \frac{v}{R_{opt}}. \tag{13}$$

In Equation 13, the optimal resistance is computed from the expression (Guyomar, Badel, Lefeuvre, & Richard, 2005),

$$R_{opt} = \frac{1}{C_o \omega} \tag{14}$$

where C_o is the capacitance of the material used and ω is the angular frequency of the device. Using Equations 12 through 14, the amount of power provided from each piezoelectric device when subjected to dynamic

Figure 7
(a) Output Voltage Versus Time for an APC Stripe Actuator (40-1010). The Output Voltage is Induced from Mechanical Vibration Loading Experienced by a Washing Machine, Dryer, and Microwave Oven. (b) Output Voltage Versus Time for a MIDE Quickpack Actuator (qp20w). The Output Voltage is Induced from Mechanical Vibration Loading Experienced by a Washing Machine, Dryer, and Microwave Oven

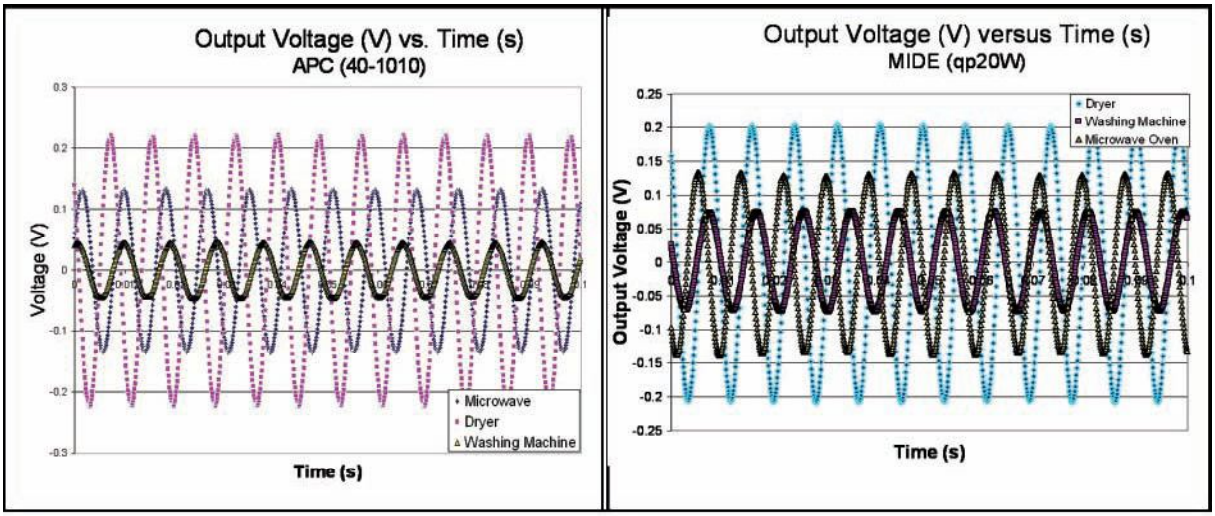

Table 6
Physical and Electromechanical Properties of (a) APC Device (40-1010) and (b) MIDE Device (qp20w)

MIDE, qp20w	clothes dryer	washing machine	microwave oven
maximum voltage induced (V)	0.20	0.08	0.13
surface area sides (m^2) (# of devices in array)	1.50 (38750)	1.42 (36683)	0.26 (6716)
surface area of top (m^2) (# of devices in array)	0.49 (253)	N/A (top loaded machine)	0.20 (103)
total power generated (mW)	185	103	5.66
energy generated per month (mWh/month)	76300	31800	6780

APC International, 40-1010	clothes dryer	washing machine	microwave oven
maximum voltage induced (V)	0.22	0.05	0.13
surface area sides (m^2) (# of devices in array)	1.50 (5410)	1.42 (4730)	0.26 (867)
surface area of top (m^2) (# of devices in array)	0.49 (408)	N/A (top loaded machine)	0.20 (167)
total power generated (mW)	68.6	2.42	3.98
energy generated per month (mWh/month)	2360	62.4	39.8

loading from either a washing machine, dryer, or microwave was calculated. The measures are presented in Table 6. Although the output power of both piezoelectric bimorphs were small (e.g., between 0.5 and 12.7 μW and 2.8 and 30.1 μW for APC and MIDE, respectively), we have incorporated these devices into arrays to obtain larger output power values.

Specifically, commercially available appliances were selected for the study: a GE 3.2 cu. ft. super capacity washer, GE 7.0 cu. ft. 6-cycle super capacity electric dryer, and GE 1.1 cu. ft. capacity countertop microwave oven. We have calculated the maximum number of piezoelectric devices that can be cantilever mounted to the top and side surfaces of the appliances. This was done by dividing the available surface area of each appliance by the surface area of the actuator (assuming cantilever mounting). The maximum number of piezoelectric devices was multiplied by the amount of power produced by one bimorph device. The results from these calculations are provided in Table 6.

The amount of harvested energy provided by the washer, dryer, and microwave from the APC array of devices for one household was 62.4, 2360, and 39.8 mWh per month, respectively. And the amount of energy harvested from the MIDE device for one household for the washer, dryer, and microwave was 31800, 76300, and 6780 per month, respectively. The results obtained from this case study demonstrate the opportunity for scavenging vibration energy from these devices and provide a reasonable argument for additional focus on design and development of advanced materials that

are more suitable for this form of regenerative energy. In fact, if this technology were applied to every washer, dryer, and microwave in every household in Pennsylvania (4.86 million; Day, 1996), then ~144.8 MWh (494 MBtu) and ~559 MWh (1907 MBtu) of energy could be captured from arrays of APC and MIDE devices, respectively, in 1 year.

4. Critical Areas of Development for Realization of Commercial Devices

The realization of commercial energy-harvesting piezoelectric devices necessitates advancement in several key areas. First, the inherent brittleness of ceramic piezoelectric materials limits the size of piezoelectric devices. In theory, larger deflections and sizes of piezoelectric devices produce enhanced power. However, larger devices are subject to catastrophic brittle failure as the lengths of beams increase, and larger deflections fatigue materials more rigorously than smaller deflections. Investigations of composite materials, for example, piezoelectric polymers with embedded piezoelectric materials and multiple-layered devices with higher values of brittle toughness, are warranted. Information obtained from these studies will be used to determine critical aspect ratios for geometry of piezoelectric devices that will ultimately be used for both single and multidevice (array) systems.

To address the challenge of weak fracture toughness of piezoelectric ceramics, studies addressing the (a) optimization of design geometry, for example, aspect ratios for cantilever beam structures, and (b) methodology for designing arrays of devices for enhanced charge density and lifetime time are needed.

In our case study on household appliances, arrays of commercial PZT-5H bimorph piezoelectric structures were used; however, the implication of increased complexity and probability of increased failure due to enhanced complexity were not addressed but are, nevertheless, an important area for future study. So, studies focusing on optimization of the number of devices of a given size within an array system are recommended.

A myriad of PZT-5H materials are commercially available for both sensor and actuator applications; however, a number of novel piezoelectric materials could potentially be equally or better suited to energy-harvesting applications. Relaxor-type ferroelectrics such as single crystals of $Pb(Mg_{1/3}Nb_{2/3})O_3$ (PMN), $Pb(Zn_{1/3}Nb_{2/3})O_3$ (PZN) and binary systems of these systems coupled with $PbTiO_3$ (PT), PMN-PT, and PZN-PT could pave the way towards commercially affordable sustainable piezoelectric energy-harvesting systems with higher output power capabilities. These materials differ from traditional ferroelectric materials because they have a broad phase transition from a paraelectric to ferroelectric state, dielectric relaxation, and weak remanent polarization. The advantages of these materials are their large coupling coefficients and large piezoelectric constants, and high strain levels, which are higher than many piezoelectric ceramic materials. PMN-PT single crystals also have high longitudinal electromechanical coupling factors, which are 90% greater than PZT (Zhang et al., 2003).

Lifetime prediction as a function of acceleration and frequency must be investigated for the application of piezoelectric materials as energy-harvesting devices. The majority of these devices are several millimeters in size and typically operate subjected to either 33 or 31 loading. Lifetime predictions for most axially loaded (33 loading) devices tend to be lengthy (e.g., in excess of 4 years in comparison to transversely loaded devices). Piezoelectric actuator lifetime in terms of electrical performance has been studied as a function of temperature, preload, humidity, poling, and driving signal. Resistance degradation and lifetime characteristics of PZT thin films have also been investigated and found to exhibit both power-law voltage and Arrhenius temperature dependence (Al-Shareef & Dimos, 1997). Crack growth rates due to cyclic and static mechanical loading as a function of poling have also been studied (Salz, Hoffman, Westram, & Rödel, 2005), but it is unclear whether the same mechanical loading and electromechanical degradation experienced by sensors and actuators are identical for energy-harvesting applications. Specifically, factors crucial for determining energy-harvesting device lifetime—frequency, acceleration, and duty cycle—are conspicuously absent in previous studies (He, Loh, & Ong, 2005; Jones, Salz, & Hoffman, 2005; Li, Rowe, Inclan, & Mamishev, 2006). Instead, the majority of the studies on electromechanical behavior of piezoelectric materials have focused on the effects of voltage, structural fatigue, and environmental factors such as temperature, humidity, and so on.

Lastly, development of design strategies for self-energizing and energy-harvesting piezoelectric devices is needed because their usage and application differ from sensors and actuators. Notable algorithms for the design of power system (Cook, Albano, Nevius, & Sastry, 2006; Cook & Sastry, 2005) sensor and actuator systems have been developed (Rader,

Afagh, Yousefi-Koma, & Zimcik, 2007), but none for sustainable piezoelectric energy-harvesting systems. Typically, duty cycle, force and/or displacement, power factor, precision, accuracy, repeatability, efficiency, and actuator response speed are key design drivers for sensor and actuator design. But, the application of the same design approaches to energy-harvesting applications is dubious. For example, in the case of energy-harvesting devices, high charge density for energy transmittal to capacitors and batteries is essential, indicating the need for advancement in signal processing techniques, while displacement and micro-strain are key parameters for design sensor applications.

5. Conclusions and Future Work

The potential for piezoelectric energy-harvesting systems is great and spans many industries and sectors, including self-energizing MEMS; sensor and biomedical structural applications; and regenerative energy harvesting including vehicles, engineering structures, and household appliances. The sustainable energy-harvesting devices for engineering structures and household devices could ultimately be used to supply power to the grid. Material development and development of design approaches are currently being pursued to improve the capabilities for energy-harvesting devices. Our future work will include optimization of the design of a self-energizing indentation and shear modulus measurement device; development of an algorithm for the strategic design of sustainable piezoelectric energy-harvesting devices; and development of mathematical models to predict the lifetime of commercial piezoelectric materials as a function of frequency and acceleration.

References

Al-Shareef, H. N., & Dimos, D. (1997). Leakage and reliability characteristics of lead zirconate titanate thin-film capacitors. *Journal of the American Ceramic Society*, *80*(12), 3127-3132.

Allen, J. J., & Smits, A. J. (2001). Energy harvesting eel. *Journal of Fluids and Structures*, *15*(3/4), 629-640.

APS. (2008, May 8). *Appliance usage information*. Retrieved September 3, 2008, from http://www.aps.com/aps_services/residential/waystosave/ResWaystoSave_24.html

Beeby, S. P., Torah, R. N., Tudor, M. J., Glynne-Jones, P., O'Donnell, T., Saha, C. R., et al. (2007). A micro electromagnetic generator for vibration energy harvesting. *Journal of Micromechanics and Microengineering*, *17*(7), 1257-1265.

Cho, J., Anderson, M., Richards, R., Bahr, D., & Richards, C. (2005a). Optimization of electromechanical coupling for a thin-film PZT membrane: I. Modeling. *Journal of Micromechanics and Microengineering*, *15*(10), 1797-1803.

Cho, J., Anderson, M., Richards, R., Bahr, D., & Richards, C. (2005b). Optimization of electromechanical coupling for a thin-film PZT membrane: II. Experiment. *Journal of Micromechanics and Microengineering*, *15*(10), 1804-1809.

Cook, K. A., Albano, F., Nevius, P. E., & Sastry, A. M. (2006). POWER (power optimization for wireless energy requirements): A MATLAB based algorithm for design of hybrid energy systems. *Journal of Power Sources*, *159*(1), 758-780.

Cook, K. A., & Sastry, A. M. (2005). An algorithm for selection and design of hybrid power supplies for MEMS with a case study of a micro-gas chromatograph system. *Journal of Power Sources*, *140*(1), 181-202.

Cook-Chennault, K. A., Thambi, N., & Sastry, A. M. (2008). Powering MEMS portable devices—A review of non-regenerative and regenerative power supply systems with special emphasis on piezoelectric energy harvesting systems. *Smart Materials & Structures*, *17*(4).

Day, J. C. (1996). *Projections of the number of households and families in the United States: 1995 to 2010* (U.S. Census Bureau, Current Population Reports, P25-1129). Washington, DC: Government Printing Office.

Energy Information Administration. (2002). *Consumption of energy for all purposes by manufacturing industry and region*. Retrieved 2007 from http://www.eia.doe.gov/emeu/mecs2002/data02/pdf/table1.2_02.pdf

Energy Information Administration. (2006). *Total energy consumption by major fuel for all buildings*. Retrieved 2007 from http://www.eia.doe.gov/emeu/cbecs/cbecs2003/detailed_tables_2003/2003set14/2003html/c1a.html

Engel, T. G., Keawboonchuay, C., & Nunnally, W. C. (2000). Energy conversion and high power pulse production using miniature piezoelectric compressors. *IEEE Transactions on Plasma Science*, *28*(5), 1338-1341.

Guyomar, D., Badel, A., Lefeuvre, E., & Richard, C. (2005). Toward energy harvesting using active materials and conversion improvement by nonlinear processing. *IEEE Transactions on Ultrasonics, Ferroelectrics, and Frequency Control*, *52*(4), 584-595.

He, Z. M., Loh, H. T., & Ong, E. H. (2005). A probabilistic approach to evaluate the reliability of piezoelectric microactuators. *IEEE Transactions on Reliability*, *54*(1), 83-91.

Jeon, Y. B., Sood, R., Jeong, J. H., & Kim, S. G. (2005). MEMS power generator with transverse mode thin film PZT. *Sensors and Actuators A: Physical*, *122*(1), 16-22.

Jones, J. L., Salz, C. R. J., & Hoffman, M. (2005). Ferroelastic fatigue of a soft PZT ceramic. *Journal of the American Ceramic Society*, *88*(10), 2788-2792.

Keawboonchuay, C., & Engel, T. G. (2003). Maximum power generation in a piezoelectric pulse generator. *IEEE Transactions on Plasma Science*, *31*(1), 123-128.

Keawboonchuay, C., & Engel, T. G. (2004). Scaling relationships and maximum peak power generation in a piezoelectric pulse generator. *IEEE Transactions on Plasma Science*, *32*(5), 1879-1885.

Kim, C.-W., Jung, S. N., & Choi, J. H. (2008). Automotive structure vibration with component mode synthesis on a multi-level. *International Journal of Automotive Technology*, *9*(1), 119-122.

Kim, H. W., Batra, A., Priya, S., Uchino, K., Markley, D., Newnham, R. E., et al. (2004). Energy harvesting using a

piezoelectric "cymbal" transducer in dynamic environment. *Japanese Journal of Applied Physics: Part 1—Regular Papers, Short Notes & Review Papers*, *43*(9A), 6178-6183.

Lee, H. J., & Saravanos, D. A. (1998). The effect of temperature dependent material properties on the response of piezoelectric composite materials. *Journal of Intelligent Material Systems and Structures*, *9*(7), 503-508.

Li, X. B., Rowe, G., Inclan, V., & Mamishev, A. V. (2006). Nondimensionalized parametric modeling of fringing electric-field sensors. *IEEE Sensors Journal*, *6*(6), 1602-1608.

Mateu, L., & Moll, F. (2005). Optimum piezoelectric bending beam structures for energy harvesting using shoe inserts. *Journal of Intelligent Material Systems and Structures*, *16*(10), 835-845.

Miles, R. W., Hynes, K. M., & Forbes, I. (2005). Photovoltaic solar cells: An overview of state-of-the-art cell development and environmental issues. *Progress in Crystal Growth and Characterization of Materials*, *51*(1-3), 1-42.

Miles, R. W., Zoppi, G., & Forbes, I. (2007). Inorganic photovoltaic cells. *Materials Today*, *10*(11), 20-27.

Mitcheson, P. D., Miao, P., Stark, B. H., Yeatman, E. M., Holmes, A. S., & Green, T. C. (2004). MEMS electrostatic micropower generator for low frequency operation. *Sensors and Actuators A: Physical*, *115*(2/3), 523-529.

Mitcheson, P. D., Reilly, E. K., Toh, T., Wright, P. K., & Yeatman, E. M. (2007). Performance limits of the three MEMS inertial energy generator transduction types. *Journal of Micromechanics and Microengineering*, *17*(9), S211-S216.

Myers, R., Vickers, M., Kim, H., & Priya, S. (2007). Small scale windmill. *Applied Physics Letters*, *90*(5), 3.

O'Neill, M. J., Piszczor, M. F., Eskenazi, M. I., McDanal, A. J., George, P. J., Botke, M. M., et al. (2003). The stretched lens array (SLA): A low-risk, cost-effective concentrator array offering wing-level performance of 180 W/kg and 300 w/m(2) at 300 VDC. *IEEE Aerospace and Electronic Systems Magazine*, *18*(1), 3-9.

Platt, S. R., Farritor, S., Garvin, K., & Haider, H. (2005). The use of piezoelectric ceramics for electric power generation within orthopedic implants. *IEEE-ASME Transactions on Mechatronics*, *10*(4), 455-461.

Platt, S. R., Farritor, S., & Haider, H. (2005). On low-frequency electric power generation with PZT ceramics. *IEEE-ASME Transactions on Mechatronics*, *10*(2), 240-252.

Priya, S., Chen, C. T., Fye, D., & Zahnd, J. (2005). Piezoelectric windmill: A novel solution to remote sensing. *Japanese Journal of Applied Physics: Part 2—Letters & Express Letters*, *44*(1-7), L104-L107.

Rader, A. A., Afagh, F. F., Yousefi-Koma, A., & Zimcik, D. G. (2007). Optimization of piezoelectric actuator configuration on a flexible fin for vibration control using genetic algorithms. *Journal of Intelligent Material Systems and Structures*, *18*(10), 1015-1033.

Ramsay, M. J., & Clark, W. W. (2001). *Piezoelectric energy harvesting for bio MEMS applications*. Smart Structures and Materials, Industrial Proceedings of SPIE.

Ren, K. L., Liu, Y. M., Geng, X., Hofmann, H. F., & Zhang, Q. M. (2006). Single crystal PMN-PT/epoxy 1-3 composite for energy-harvesting application. *IEEE Transactions on Ultrasonics, Ferroelectrics, and Frequency Control*, *53*(3), 631-638.

Richards, C. D., Anderson, M. J., Bahr, D. F., & Richards, R. F. (2004). Efficiency of energy conversion for devices containing a piezoelectric component. *Journal of Micromechanics and Microengineering*, *14*(5), 717-721.

Roundy, S. (2003). *Energy scavenging for wireless sensor nodes with a focus on vibration to electricity conversion*. Unpublished doctoral dissertation, University of California, Berkeley.

Roundy, S. (2005). On the effectiveness of vibration-based energy harvesting. *Journal of Intelligent Material Systems and Structures*, *16*(10), 809-823.

Roundy, S., & Wright, P. K. (2004). A piezoelectric vibration based generator for wireless electronics. *Smart Materials & Structures*, *13*(5), 1131-1142.

Roundy, S., Wright, P. K., & Rabaey, J. (2003). A study of low level vibrations as a power source for wireless sensor nodes. *Computer Communications*, *26*(11), 1131-1144.

Salz, C. R. J., Hoffman, M., Westram, I., & Rödel, J. (2005). Cyclic fatigue crack growth in PZT under mechanical loading. *Journal of the American Ceramic Society*, *88*(5), 1331-1333.

Schmidt, V. H. (1992). Piezoelectric energy conversion in windmills. *IEEE Ultrasonic Symposium*, pp. 897-904.

Secretary, I.S.B. (1987). IEEE standard on piezoelectricity. *IEEE Ultrasonics, Ferroelectrics, and Frequency Control Society*.

Shearwood, C., & Yates, R. B. (1997). Development of an electromagnetic micro-generator. *Electronics Letters*, *33*(22), 1883 1884.

Shenck, N. S., & Paradiso, J. A. (2001). Energy scavenging with shoe-mounted piezoelectrics. *IEEE Micro*, *21*(3), 30-42.

Sodano, H. A., Inman, D. J., & Park, G. (2005a). Comparison of piezoelectric energy harvesting devices for recharging batteries. *Journal of Intelligent Material Systems and Structures*, *16*(10), 799-807.

Sodano, H. A., Inman, D. J., & Park, G. (2005b). Generation and storage of electricity from power harvesting devices. *Journal of Intelligent Material Systems and Structures*, *16*(1), 67-75.

Sodano, H. A., Lloyd, J., & Inman, D. J. (2006). An experimental comparison between several active composite actuators for power generation. *Smart Materials & Structures*, *15*(5), 1211-1216.

Taylor, G. W., Burns, J. R., Kammann, S. A., Powers, W. B., & Welsh, T. R. (2001). The energy harvesting eel: A small subsurface ocean/river power generator. *IEEE Journal of Oceanic Engineering*, *26*(4), 539-547.

Umeda, M., Nakamura, K., & Ueha, S. (1996). Analysis of the transformation of mechanical impact energy to electric energy using piezoelectric vibrator. *Japanese Journal of Applied Physics: Part 1—Regular Papers, Short Notes & Review Papers*, *35*(5B), 3267 3273.

Umeda, M., Nakamura, K., & Ueha, S. (1997). Energy storage characteristics of a piezo-generator using impact induced vibration. *Japanese Journal of Applied Physics: Part 1—Regular Papers, Short Notes & Review Papers*, *36*(5B), 3146-3151.

U.S. Department of Energy & U.S. Environmental Protection Agency. (2005). *Protect the environment: Global climate change*. Retrieved September 3, 2008, from http://www.fueleconomy.gov/feg/climate.shtml

Whalen, S., Thompson, M., Bahr, D., Richards, C., & Richards, R. (2003). Design, fabrication and testing of the P^3 micro heat engine. *Sensors and Actuators A: Physical*, *104*(3), 290-298.

White, N. M., Glynne-Jones, P., & Beeby, S. P. (2001). A novel thick-film piezoelectric micro-generator. *Smart Materials & Structures*, *10*(4), 850-852.

Xue, J. G., Uchida, S., Rand, B. P., & Forrest, S. R. (2004). 4.2% efficient organic photovoltaic cells with low series resistances. *Applied Physics Letters*, *84*(16), 3013-3015.

Yang, J. (2005). *An introduction to the theory of piezoelectricity*. New York: Springer.

Yegingil, H., Shih, W. Y., & Shih, W.-H. (2007). All-electrical indentation shear modulus and elastic modulus measurement

using a piezoelectric cantilever with a tip. *Journal of Applied Physics*, *101*(5), 1-10.

Yoon, H.-S., Washington, G., & Danak, A. (2005). Modeling, optimization, and design of efficient initially curved piezoceramic unimorphs for energy harvesting applications. *Journal of Intelligent Material Systems and Structures*, *16*(10), 877-888.

Zhang, S. J., Lebrun, L., Jeong, D.-Y., Randall, C. A., Zhang, Q., & Shrout, T. R. (2003). Growth and characterization of Fe-doped Pb(Zn1/3Nb2/3)O-3-PbTiO3 single crystals. *Journal of Applied Physics*, *93*(11), 9257-9262.

Kimberly Ann Cook-Chennault, PhD, MS, is an assistant professor in the Department of Mechanical and Aerospace Engineering at Rutgers University. She received her MS degree from Stanford University and her PhD from the University of Michigan. Prior to receiving her doctorate, she worked at Ford Motor Company, Visteon, and Lawrence Livermore National Laboratory. Her lab, the Hybrid Energy Systems Laboratory, focuses on the development of strategies for the design of hybrid power systems via incorporation of battery technology and energetic materials. Her work also includes the design, optimization, and fabrication of composite piezoelectric structures.

Nithya Thambi is a BS/MS student in the Hybrid Energy Systems Laboratory at Drexel University. Her current research interests include modeling of piezoelectric energy harvesting structures.

Mary Anne Bitetto, BS, is an MS/PhD student in the Hybrid Energy Systems Laboratory at Rutgers University. She received her BS degree in mechanical engineering from The College of New Jersey (TCNJ) in Ewing. Her current research interests include the design and optimization of piezoelectric multiple-layered structures for energy-harvesting applications. She has previous experience in "green" transportation from the Vehicle Design Summit at the Massachusetts Institute of Technology where she designed and built components of Pulse, a highly efficient electric commuter vehicle. In 2004, she also worked with TCNJ's solar/electric boat team, which competes in Solar Splash, the world championship of intercollegiate solar boating.

E. B. Hameyie is a BS/MS student in civil and architectural engineering with a mechanical (HVAC) concentration from Drexel University in June 2008. She is currently a research assistant in the Hybrid Energy Systems Laboratory in the Mechanical Engineering and Mechanics Department. She is pursuing her MSc, focusing on dampening and energy-harvesting characteristics of piezoelectric materials for vibration reduction of mechanical systems. She is a student member of the American Society of Heating, Refrigerating and Air-conditioning Engineers (ASHRAE), a student member of the U.S. Green Building Council, and a member of Drexel's Chi Epsilon Civil chapter.